PHYSICAL REVIEW E **79**, 055301(R) (2009)

Anomalous scaling of three-dimensional Rayleigh-Taylor turbulence

Takeshi Matsumoto*

Division of Physics and Astronomy, Graduate School of Science, Kyoto University, Kitashirakawa-Oiwakecho, Sakyoku, Kyoto 606-8502, Japan

(Received 19 February 2009; revised manuscript received 19 March 2009; published 13 May 2009)

Three-dimensional Rayleigh-Taylor incompressible turbulence is numerically studied with the Boussinesq approximation. Our focus is on scaling properties of the moments of the density and the velocity differences (structure functions), which are directly measured from the numerical data. A comparison with the phenomenology proposed by Chertkov [Phys. Rev. Lett. **91**, 115001 (2003)] is made. It is found that deviation from the phenomenology (anomalous scaling or intermittency effect) of the density observed for high-order structure functions is quite close to that of the passive scalar with a uniform mean scalar gradient advected by the barotropic homogeneous isotropic turbulence.

DOI: 10.1103/PhysRevE.79.055301 PACS number(s): 47.27.ek, 47.27.eb, 47.27.T−, 47.55.Hd

One of the most common ways to trigger turbulence in nature is the Rayleigh-Taylor (RT) instability [1]: a heavy fluid placed on top of a light fluid under the influence of gravity is an unstable configuration. Where such a configuration occurs inevitably, turbulent state (Rayleigh-Taylor turbulence) follows, and its important consequences have been studied, particularly, in subjects related to supernova explosions [2] and inertial confinement fusion [3].

What makes elucidation of the RT turbulence challenging is that statistics of its fluctuations depend on time, which is markedly different from conventional study on statistically steady-state turbulence [4]. Nevertheless there is a universal law about this time-dependent nature of RT turbulence. This law states that the largest length scale of RT turbulence [here called the mixing zone length $L(t)$, indicated in Fig. 1] grows as the square of time,

$$L(t) = C_F A g t^2, \tag{1}$$

as long as boundary effects are negligible (see, e.g., [5]). Here A is the Atwood number, measuring the density difference between the top and bottom layers $A=(\rho_{\mathrm{top}}-\rho_{\mathrm{bottom}})/(\rho_{\mathrm{top}}+\rho_{\mathrm{bottom}})$, g is the gravitational acceleration, and C_F is thought to be a universal constant. By using this mixing zone length, $L(t)$, Chertkov developed a phenomenology of RT turbulence in the case of small density differences [6]. It predicts not only spatial but also temporal scalings for the velocity and the density fluctuations in both two and three spatial dimensions. Subsequent to this phenomenology, there has been a series of numerical studies regarding the statistical properties of RT turbulence and its universality.

For the two-dimensional (2D) case, this prediction was later confirmed through a numerical simulation by Celani *et al.* [7], and deviation from the phenomenological prediction is observed in high-order statistics as expected. For the three-dimensional (3D) case, the prediction for the velocity statistics and its universality was extensively studied by Boffetta *et al.* [8], and the internal structure within the mixing zone was studied by Vladimirova and Chertkov [9]. Employing a method similar to those in [7,8], we perform a numerical simulation of RT turbulence in the three-dimensional space and test the phenomenology [6]. Our main target is the statistics of the density. In particular we present them in a way as simple as possible.

Chertkov's phenomenology predicts for the 3D RT turbulence that the velocity and density increments over distance r in the inertial range at an equal time t obey the following scaling laws in r and t:

$$\delta_r u \sim \epsilon_r(t)^{1/3} r^{1/3} \sim u_L(t) \left[\frac{r}{L(t)}\right]^{1/3} \sim (Ag)^{2/3} r^{1/3} t^{1/3}, \tag{2}$$

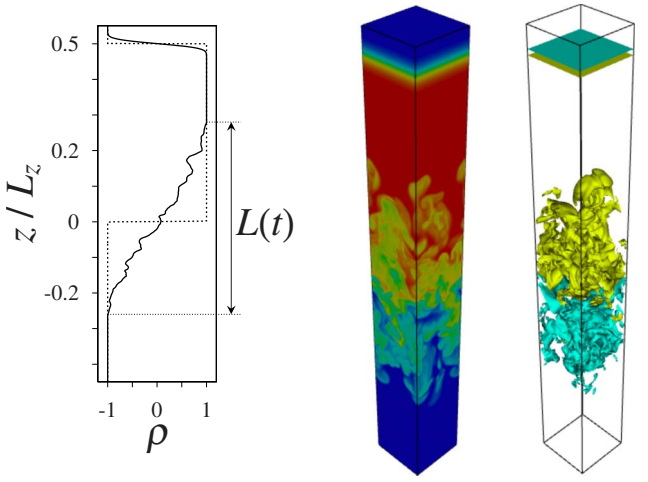

FIG. 1. (Color online) Left: horizontally averaged instantaneous density profile. The direction of the gravity is from top to bottom. The dashed line is the initial profile. The mixing zone length $L(t)$ is determined from the horizontally averaged density profile. Middle 3D plots of the instantaneous density in the whole computational domain. High (low) density is coded red/gray (blue/dark). Right: the yellow/gray and blue/dark isosurfaces of the density correspond values $\rho=0.4,-0.4$, respectively. Note that the upper density interface at $z=0.5$, which is needed to conform to periodicity, does not become turbulent.

*takeshi@kyoryu.scphys.kyoto-u.ac.jp

$$\delta_r \rho \sim \chi_r(t)^{1/2} \epsilon_r(t)^{-1/6} r^{1/3} \sim \Delta\rho \left[\frac{r}{L(t)}\right]^{1/3}$$

$$\sim \Delta\rho (Ag)^{-1/3} r^{1/3} t^{-2/3}. \quad (3)$$

Here it is assumed that the energy and density dissipation rates at small length scale r become instantaneously equal to those at the largest scale $L(t)$ (adiabaticity): $\epsilon_r(t) \sim \epsilon_{L(t)} \sim u_L(t)^3/L(t)$ and $\chi_r(t) \sim \chi_{L(t)} \sim (\Delta\rho)^2/t$. And $u_L(t)$ is the largest-scale velocity given by $u_L(t) \sim L(t)/t$, and $\Delta\rho = \rho_{\text{top}} - \rho_{\text{bottom}}$ is the density difference at the largest scale. This is a generalization of the statistically steady-state turbulence phenomenology to that of the unsteady RT turbulence. Notice that the temporal scalings in the rightmost-hand sides of Eqs. (2) and (3) are the result of Eq. (1). The first lines of Eqs. (2) and (3) are actually independent on how $L(t)$ grows in time. We shall here calculate second-, fourth-, and sixth-order moments of $\delta_r \rho$ and $\delta_r u$ (structure functions) from the numerical simulation and compare their scaling exponents to the prediction [Eqs. (2) and (3)]. The emphasis is on anomalous scaling, that is, how higher-order structure functions deviates from the phenomenological prediction.

The initial condition in our numerical simulation is that the velocity is zero everywhere $\boldsymbol{u}(\boldsymbol{x}, t=0) = \boldsymbol{o}$, and the density varies as a step function of the vertical coordinate z, $\rho(\boldsymbol{x}, t=0) = \rho_{\text{top}}(z>0), \rho_{\text{bottom}}(z<0)$. We consider the case that the density difference is small, which amounts to small Atwood number $A \ll 1$ cases. We solve the equations with Boussinesq approximation which is valid for small Atwood number cases

$$\partial_t \boldsymbol{u} + (\boldsymbol{u} \cdot \boldsymbol{\nabla})\boldsymbol{u} = -\boldsymbol{\nabla} p + A\rho \boldsymbol{g} + \nu \boldsymbol{\nabla}^2 \boldsymbol{u}, \quad \boldsymbol{\nabla} \cdot \boldsymbol{u} = 0, \quad (4)$$

$$\partial_t \rho + (\boldsymbol{u} \cdot \boldsymbol{\nabla})\rho = \kappa \boldsymbol{\nabla}^2 \rho. \quad (5)$$

Here the variables (p pressure, $\boldsymbol{g}$ gravitational acceleration, ν kinematic viscosity, and κ density diffusivity) are suitably normalized so that the initial density is now $\rho = 1 (z>0)$, $-1 (z<0)$. The Atwood number is set as $A=0.15$. We assume that ν and κ are the same for the top ($z>0$) and bottom ($z<0$) fluids. The Prandtl number $Pr = \nu/\kappa = 1$ is considered here. The numerical scheme is a standard spectral method with a fourth-order Runge-Kutta scheme for time advancement. The alias error is removed by the phase-shift method. The boundary condition is triply periodic in the domain size $(4\pi)^2 \times 32\pi$ with grid points $256^2 \times 2048$. We stop the simulation when the mixing zone length reaches $0.75 L_z$, where L_z is the vertical domain size. Ensemble average is taken over 20 different initial 2D random perturbations added to the initial density interfaces. This simulation strategy is basically the same as in [7,8]. Simulation with a smaller domain $(2\pi)^2 \times 16\pi$ with $128^2 \times 1024$ is also performed. Comparison between the two sizes suggests robustness of the results presented here.

First of all, we check whether or not the t^2 law [Eq. (1)] holds in our simulation since it is a key input for the phenomenology. We define here the mixing zone length $L(t)$ as a z zone where $-0.99 \le \bar{\rho}(z,t) \le 0.99$ [$\bar{\rho}(z,t)$ is the horizontally averaged density, see Fig. 1]. The ensemble averaged mixing zone length $\langle L(t) \rangle$ is shown in the inset of Fig. 2. The t^2 scaling law is hardly seen, a well-known effect of subdominant corrections [5,10]. Nevertheless it is estimated that the effective scaling law is $t^{1.3}$, which has an important consequence when we discuss the temporal scaling of the structure functions. In order to see whether or not the leading behavior t^2 exists, we apply the method proposed in Ref. [10] to our data: if Eq. (1) holds for the ensemble-averaged mixing zone length $\langle L(t) \rangle$, then the graph of $[(d/dt)\langle L(t) \rangle]^2/[4Ag\langle L(t) \rangle]$ becomes flat and its value is the constant C_F in Eq. (1). Indeed as shown in Fig. 2 the graph becomes roughly flat in the range $30 < t < 60$. This implies that the t^2 [Eq. (1)] is the leading term there. Within this time range we shall later analyze a temporal scaling behavior of the structure functions. Here the value the universal constant C_F obtained from the flat region in Fig. 2 is around 0.04 which is consistent to the value 0.048 reported in [10] and 0.038 in [8]. However it is quite different from the value 0.12 for the 2D case measured in [7].

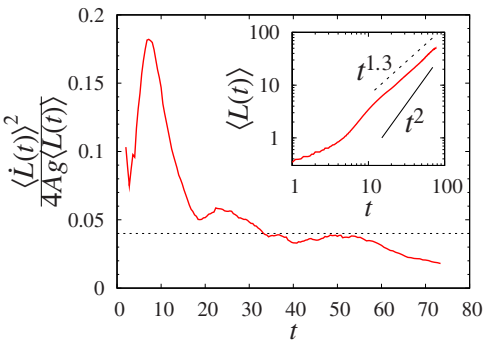

FIG. 2. (Color online) If the graph becomes flat, the flat value corresponds to that of the constant C_F in Eq. (1) [10]. Here $\langle L(t) \rangle$ is the ensemble averaged mixing zone length. Inset: $\langle L(t) \rangle$ in log-log scale. The effective scaling law of $\langle L(t) \rangle$ is close to $t^{1.3}$.

Now we show in Fig. 3 the structure functions of the density and the velocity as functions of spatial scale for a fixed time. They are spatially averaged within the mixing zone. Here the fixed time $t=57.0$ is chosen as roughly the latest time when the indicator shown in Fig. 2 is flat ($30 < t < 60$). During this time range, the spatial scaling behavior of the structure functions does not change but the spatial inertial range broadens as the time elapses. For the second-order moments, the scaling exponents of the density and the velocity structure functions are close to the dimensional predictions [Eqs. (2) and (3)], which is the same result as [8]. This supports the argument in Ref. [6] that the RT turbulence in 3D obeys the Kolmogorov-Obukhov-Corrsin scaling, implying that the density in the inertial range behaves as a passive scalar. For the fourth and sixth orders, the scaling exponents of the density structure functions deviate from the phenomenology. Following the method in Ref. [7] for the 2D RT turbulence case, we compare these anomalous scaling exponents obtained here with those of the passive scalar with a mean scalar gradient advected by steady, homogeneous, and isotropic turbulences without the gravity effect [11]. As shown in Fig. 3(a) the density scaling exponents in r observed here are quite close to those calculated in Ref. [11] of the passive scalar. In contrast, the scaling exponents of the velocity obtained here do not clearly exhibit such agreement

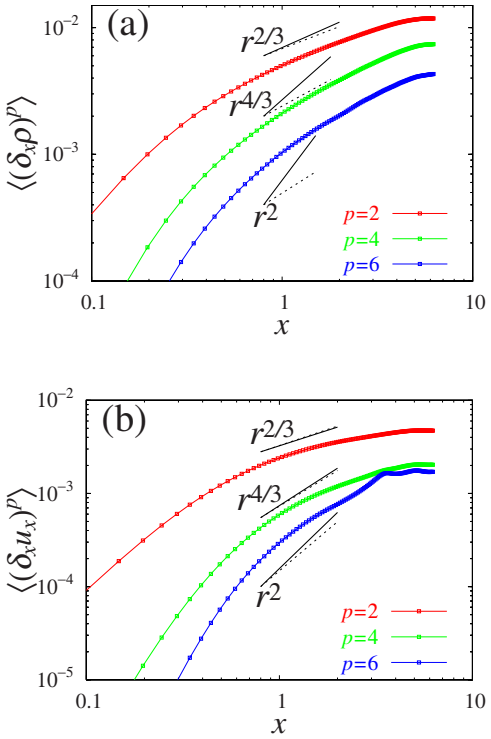

FIG. 3. (Color online) (a) Density structure functions $\langle \delta_x \rho^p \rangle$ as functions of distance x along the horizontal x coordinate at fixed time $t=57.0$. (b) Same as (a) but for longitudinal velocity structure functions $\langle \delta_x u_x^p \rangle$, where u_x is the x component of the velocity. Solid lines for both panels represent the phenomenological predictions [Eqs. (2) and (3)]. Dashed lines represent the anomalous exponents of the passive scalar with a mean scalar gradient obtained in [11] and of the homogeneous isotropic turbulent velocity in [12].

with those of the homogeneous isotropic turbulence (for example, with the exponent values given in Ref. [12]). The possible reason for this may be that the inertial range is not wide enough. In Ref. [8], with the aid of the extended self similarity (ESS) analysis, such agreement for the velocity is firmly observed. Concerning the isotropy of the structure functions as functions of r, we show the density structure functions for the three different increments in Fig. 4. For the vertical increments, we subtract the linear variation in z due to the mixing zone growth $[\Delta\rho/L(t)]z$ (mean density gradient contribution). It is seen that the scaling exponents in the inertial range are rather close for the three directions. However difference in the dissipation range is enhanced for $p=4,6$. For the longitudinal velocity structure functions, both horizontal components $\delta_x u_x, \delta_y u_y$ agree well but the horizontal component $\delta_z u_z$ is quite different from the two others (figure not shown).

Let us move to temporal scaling of the density and the velocity structure functions. In Fig. 5 we plot the structure functions as function of time t for a fixed spatial scale $r=1.23$. This spatial scale within the inertial range is chosen based both on the scaling range shown in Fig. 3 and on the constancy of the kinetic-energy flux (figure not shown). The temporal scaling behavior does not change much for $1.0 \le r \le 2.0$. As already discussed, the "inertial range in time" is expected for $30 < t < 60$ (see the flat region in Fig. 1). As

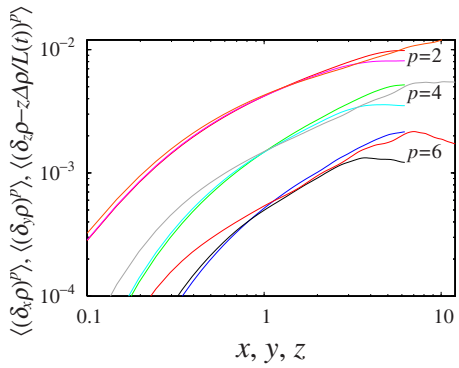

FIG. 4. (Color online) Density structure functions for horizontal (x,y) and vertical (z) increments at fixed time $t=57.0$. For the vertical ones, the density variations due to the mean gradient $\Delta\rho/L(t)$ are subtracted. Longer curves correspond increments along z direction. (Graphs are suitably shifted in the ordinate direction.)

shown in Fig. 5 the density and the velocity structure functions exhibit a reasonable scaling behavior during this time range. The temporal scaling exponents for the density seen here are at first sight different from the prediction [Eq. (3)]. However there is an interpretation of this. Remember that in the derivation of Eq. (3) we have $\delta_r \rho \sim \Delta\rho[r/L(t)]$. We can put the effective scaling law $\langle L(t) \rangle \propto t^{1.3}$ into this relation. As

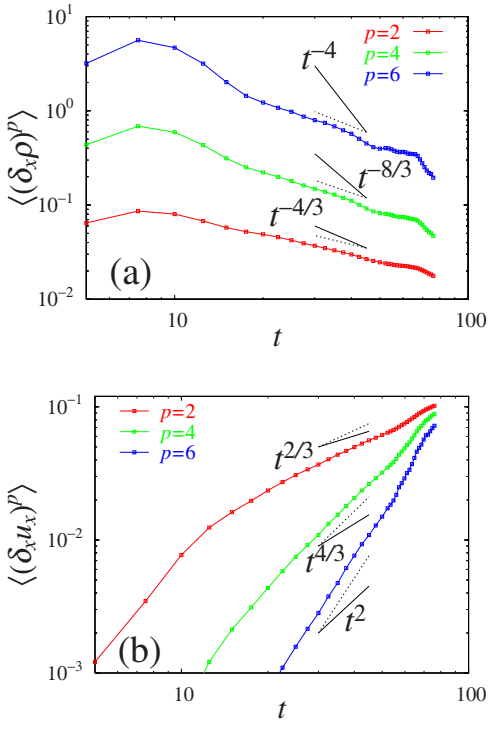

FIG. 5. (Color online) (a) Density structure functions $\langle \delta_x \rho^p \rangle$ as functions of time at the fixed spatial scale $x=1.23$. Solid lines represent the phenomenological predictions. Dashed lines represent exponents $-1.3\xi_p (p=2,4,6)$, where 1.3 is the effective scaling exponent of the mixing zone length $L(t)$ (see Fig. 1) and ξ_p are the anomalous exponents of the passive scalar structure functions with a uniform mean scalar gradient obtained in [11]. (b) Same as (a) but for longitudinal velocity structure functions $\langle (\delta_x u_x)^p \rangle$. Here dashed lines represent fits by eyes $[1.0(p=2), 2.1(p=4), 3.3(p=6)]$.

a result the temporal exponents of the density structure functions of all p's presented here agree with the relation $\langle(\delta_r\rho)^p\rangle \sim (\Delta\rho)^p[r/L(t)]^{\xi_p} \propto t^{-1.3\xi_p}$. Here 1.3 is the effective temporal scaling exponent of $\langle L(t)\rangle$ and ξ_p is the anomalous scaling exponents of the pth-order structure functions of the passive scalar with a mean scalar gradient advected by the barotropic homogeneous isotropic turbulence ($\xi_2=0.578, \xi_4=0.822, \xi_6=0.950$) [11]. This agreement suggests $\langle(\delta_r\rho)^p\rangle \propto [r/L(t)]^{\xi_p}$. For the second order, the exponent ξ_2 is not very far away from the phenomenological prediction $[r/L(t)]^{2/3}$. It is hence safe to say that the phenomenology [Eq. (3)] holds for the second-order moment. For the fourth- and sixth-order moments, deviation from the phenomenology [Eq. (3)] is clearly observed. The point is that how they deviate is quite similar to that of the passive scalar problem [13], namely, the saturating behavior of the exponents. Also this result indicates that the temporal scaling of the density structure function $\langle(\delta_r\rho)^p\rangle$ is involved only through $L(t)$, which may be support of the adiabaticity assumption made in the phenomenology [6] at least for the density. We point out lastly that using the effective exponent 1.3 is the same as plotting the structure functions for fixed r as a function of the mixing zone length $\langle L(t)\rangle$, as is done in Ref. [7].

For the temporal exponents of the velocity structure functions, they differ again from the dimensional prediction [Eq. (2)] even for the second order $p=2$. The second-order data grow close to t^1, which is rather different from the phenomenological prediction $t^{2/3}$. This t^1 scaling does not change if we change the spatial scale range in $1 \le r \le 2$. For the velocity, the interpretation by using the effective scaling law $\langle L(t)\rangle \propto t^{1.3}$ and the anomalous exponent of the homogeneous isotropic turbulence velocity ζ_p does not work: $\langle(\delta_r u)^p\rangle \sim u_L^p(t)[r/L(t)]^{\zeta_p} \propto t^{1.3(p-\zeta_p)-p}$ give negative temporal exponents for $p=2,4,6$. However in Ref. [8] they observed in the Fourier space that the velocity temporal scaling exponent is $t^{2/3}$ for $p=2$, which is consistent with the phenomenology. So far we do not have an explanation for these velocity temporal exponents observed here.

We draw conclusions from the numerical data about the structure functions, in particular about the density in the mixing zone. The density field of the 3D RT turbulence, which is not at all a passive scalar advected by a steady turbulent velocity, behaves in the same way as the passive scalar with a uniform mean scalar gradient advected by statistically steady homogeneous and isotropic turbulences. An interesting point in this correspondence is that the scalar mean gradient for the RT turbulence is given by $\Delta\rho/L(t)$, which is dependent on time. In Ref. [6] Chertkov pointed out that the Kraichnan model analysis [14] of the passive scalar with time-dependent statistics may be useful in understanding RT turbulence. Our result suggests that a way to incorporate this time-dependence is to consider a Kraichnan model of a passive scalar with a time-dependent mean scalar gradient $\Delta\rho/t^\beta[L(t)\sim t^\beta]$. The $\beta=2$ case corresponds formally to RT turbulence. It is also theoretically interesting to study a general exponent case β.

Recently in Ref. [8] the velocity field of RT turbulence in the mixing zone is found to have the same scaling property as the velocity of statistically steady homogeneous and isotropic turbulences. We report that the same analogy holds between the density and the passive scalar. It is remarkable that the anomalous scaling exponents of both the velocity and the density of small Atwood number RT turbulence coincide with those of the velocity and the passive scalar of 3D homogeneous isotropic turbulence.

The simulation was performed with SX-8 in Yukawa Institute for Theoretical Physics. I was supported by the Grant-in-Aid GCOE program "The Next Generation of Physics, Spun from Universality and Emergence" and the Grant-in-Aid for Exploratory Research No. 19654014 from the Japanese Ministry of Education.

[1] S. Chandrasekhar, *Hydrodynamic and Hydromagnetic Stability* (Dover, New York, 1981).
[2] A. Burrows, Nature (London) **403**, 727 (2000).
[3] S. Pfalzner, *An Introduction to Inertial Confinement Fusion* (Taylor & Francis, London, 2006).
[4] U. Frisch, *Turbulence: the legacy of A. N. Kolmogorov* (Cambridge University Press, Cambridge, 1996).
[5] J. R. Ristorcelli and T. T. Clark, J. Fluid Mech. **507**, 213 (2004).
[6] M. Chertkov, Phys. Rev. Lett. **91**, 115001 (2003).
[7] A. Celani, A. Mazzino, and L. Vozella, Phys. Rev. Lett. **96**, 134504 (2006).
[8] G. Boffetta, A. Mazzino, S. Musacchio, and L. Vozella, e-print arXiv:0902.1452.
[9] N. Vladimirova and M. Chertkov, Phys. Fluids **21**, 015102 (2009).
[10] W. H. Cabot and A. W. Cook, Nat. Phys. **2**, 562 (2006).
[11] T. Watanabe and T. Gotoh, Phys. Fluids **18**, 058105 (2006).
[12] T. Watanabe and T. Gotoh, New J. Phys. **6**, 40 (2004).
[13] Z. Warhaft, Annu. Rev. Fluid Mech. **32**, 203 (2000).
[14] G. Falkovich, K. Gawedzki, and M. Vergassola, Rev. Mod. Phys. **73**, 913 (2001).